



# **Conceptual Design and Finite Element Analysis of a Five-Minute Mini D.C Powered Air Compressor for Inflating Automobile Tyres**

**Peter Kayode Farayibi<sup>1</sup>, Oluwole Timothy Ojo<sup>1\*</sup>  
and Oluwajuwon Oluwagbemisola Caleb<sup>2</sup>**

<sup>1</sup>*Department of Industrial and Production Engineering, The Federal University of Technology,  
P.M.B.704, Akure, Ondo State, Nigeria.*

<sup>2</sup>*Department of Mechanical Engineering, The Federal University of Technology,  
P.M.B.704, Akure, Ondo State, Nigeria.*

### **Authors' contributions**

*This work was carried out in collaboration between all authors. Author PKF designed the study and managed the analyses. Author OTO did the literature searches, monitor the design analysis and wrote the first draft of the manuscript. Author OOC managed the analyses of the study and reviewed the manuscript. All authors read and approved the final manuscript.*

### **Article Information**

DOI: 10.9734/JSRR/2018/46575

Editor(s):

(1) Dr. Patricia J. Y. Wong, Nanyang Technological University, School of Electrical and Electronic Engineering, Singapore.

Reviewers:

(1) Carlos Alberto Ferreira Lagarinhos, Polytechnic School of the University of São Paulo, Brazil.

(2) J. Dario Aristizabal-Ochoa, National University of Colombia, Colombia.

Complete Peer review History: <http://www.sdiarticle3.com/review-history/46575>

**Original Research Article**

**Received 19 October 2018**  
**Accepted 09 January 2019**  
**Published 23 January 2019**

## **ABSTRACT**

In this study, a Five-minute DC powered tyre inflator has been successfully designed. The machine was designed to satisfy a tyre specification of R205/65R15 95H because it is widely used by both private and commercial vehicle users. The design has two units; the compressor side and the electric motor side. The components of the compressor side include; piston, crank shaft, cylinder, cylinder head, rings, crank case, valves, pressure gauge and four studs. The design analysis of the reciprocating parts, connecting rod and crank shaft was done and structural integrity of the members evaluated using Finite Element modelling tool in Solidworks CAD application. Under the action of 155 N load on top of the piston, the simulation result indicates that a maximum stress of  $3.7 \times 10^6 \text{ N/m}^2$  was reached along the fillet neck of the connecting rod, and this value is lower than the yield strength of the material used which is  $4.7 \times 10^8 \text{ N/m}^2$ . The strength worthiness with

\*Corresponding author: E-mail: [wolox025@gmail.com](mailto:wolox025@gmail.com);

respect to slenderness ratio of the connecting rod was confirmed by the buckling analysis with a shape factor of 0.8. Upon the subjection of the crank shaft to a load of 155 N acting normally to the crank pin, the shaft experienced a negligible resultant displacement of  $9.8 \times 10^{-5} \text{ mm}$  and a maximum stress of  $2.48 \times 10^6 \text{ N/m}^2$  with a minimum factor of safety of  $2.5 \times 10^2$  indicating that the crank shaft design is appropriate. The volumetric efficiency is found to be 80% while the working efficiency is 62.5%. The conceptual design is considered fit for fabrication based on the design analysis and evaluation.

*Keywords: Design; DC powered; tyre inflator; finite element analysis; automobile tyre.*

## 1. INTRODUCTION

The automobile sector plays a big role in the economics of all the countries of the world. One of the most critical problems of vehicle is the correct performance of the tyre. Making sure that tyres are inflated for the right amount of pressure for the load being carried and for the right road condition can lead to preservation of tyres and this will generally result into optimal vehicle operation without any risk [1].

Often times, many car/ vehicle owners inflate tyres without a recourse to the recommended optimum inflation pressure for specific cars. Correct tyre inflation is of great importance not only to service life of the tyre but also economic, handling characteristics and the safety of the tyre and human life. Driving an under-inflated tyre has serious negative consequences on tyre durability, steering response, directional stability, fuel efficiency which impacts on higher rolling resistance and low mileage. According to America Automobile Association, 80% of Vehicles have at least one under inflated tyre and when the pressure of the tyre is below 2 psig than the ideal pressure, the fuel efficiency is reduced by 10% [2].

Worthy of note is the fact that incorrect inflation of pressure in tyre affects vehicle handling, passenger's comfort, braking conditions, reduction in fuel economy as well as tyre life span. Hence, there is a great need to pay serious attention to tyre pressure condition [3].

Wheel being one of the major parts of an automobile vehicle, comprises tyre and rim in which the tyre is filled with compressed air. The pressure of tyre contributes significantly to the overall efficiency of automobile vehicles and must be kept within the prescribed range. Inflation of tyres is done by the help of an air compressor also known as inflator. An air compressor is a device that converts power into potential energy by forcing air into a smaller

volume and thus increasing its pressure [4]. Finite Element analysis as a powerful and economic method has been used widely for Engineering designs [5].

The importance of Central Tyre Inflation (CTI) system which permits a vehicle operator to optimize tyre and vehicle performance by varying inflation pressures in response to changing operating conditions such as load being carried, road condition and vehicle speed while the vehicle is in motion was emphasized by [6].

In order to improve the efficiency of vehicles, a good number of researchers have worked and many are still working on the development of devices for inflating automobile tyres, bearing in mind that inflation affects stability of vehicles [7].

Kayisoglu et al. [8] developed an automatic tyre pressure control system to improve the tractive efficiency of tractors. The developed system was designed in a flexible structure which can be adapted to all brand and model of tractors. With the automatic tire pressure control system, occurrence of negative traffic effects on the field could be minimized.

Latha et al. [9] researched on solar based air compressor for inflating tyres. Solar photo voltaic was used to generate power needed to run the air compressor used for inflating tyres. Mushiri et al. [10] designed an automatic tyre pressure inflation system for small vehicles. The developed system was monitored and controlled by a Java/Android program which detects low pressure and initiates compressor On / Off states.

For the purpose of minimizing the avoidable stress, inconveniences and time wastage often experienced by drivers when tyres are deflated, Rathi et al. [11] designed an automatic central air inflation system which could display on an LCD screen the optimal level of car tyre while

been inflated as well as tyre pressure level when in running condition. Farayibi [12] used finite element analysis to evaluate the integrity of a conceptual design on plastic recycling machine for the production of thin filament coil.

Putting into consideration time factor and availability of an air filled station most especially while on a long journey, it is obvious that the existing way of maintaining the pressure level of an automobile vehicle tyre is too tedious. The problem will be more complex and dynamic if the tyre pressure level can no longer sustain the vehicle in motion in addition to an already deflated spare tyre along an area where people do not live. The design presented in this work is therefore geared towards improving the efficiency of automobile tyres and reducing cost as well as time spent in looking for gas filling stations whenever vehicle tyre got deflated. In other word, the overall efficiency of an automobile depends on the tyres pressure gauge. Thus, the need arises for a mini and mobile D.C powered air compressor.

## 2. MATERIALS AND METHODS

### 2.1 Design Concept Description

A five-minute D.C powered automobile tyre air compressor is a mobile reciprocating air compressor, powered through 12 volts D.C source and delivers compressed air at 50 kpsig after been trapped and compressed in the compression chamber for inflation of automobile tyre just in five minutes. It consists of two units; the electric and the compressor units. The air compressor section, located in front of the electric motor, is made up of the cylinder head, cylinder, piston, rings, crankshaft, crankcase

and crankcase cover. Two holes of different diameters are machined on the cylinder head, guided by inlet and outlet valve situated at bottom and top side of the cylinder head respectively. A flexible quarter-circle shape shim-steel flap embedded into the cylinder head was chosen as the inlet valve. It was screw to the cylinder head using a regular flat head thread screw. To prevent pressure losses, a polymer O-Ring was recessed into the cylinder head, ensuring air-tight between the shim-steel and the aluminium cylinder head. Another O-Ring was used for the purpose of air-tighten around the neck of the cylinder head, in between the cylinder head and the cylinder as shown in Fig. 2 which presents the assembly view of the machine with the list of its major part while the component parts are listed in Table 1.

The two sides were coupled together with the aid of spur gear arrangement. The gear was chosen as the coupling method in order to enhance accurate and exact power transmission at a gear ratio of 1:1.

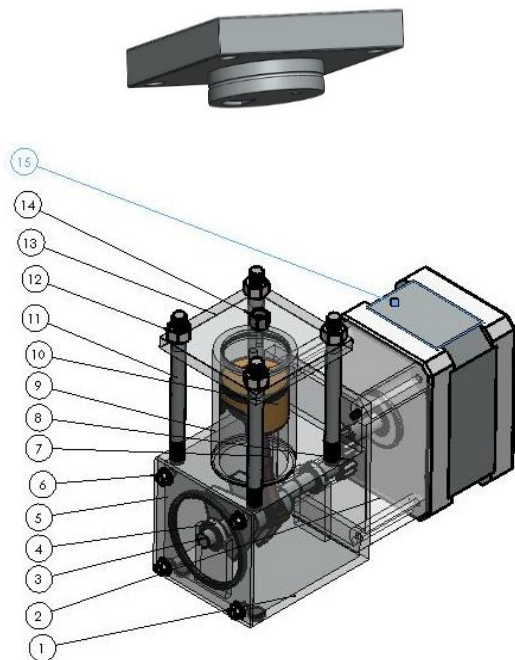
The cylinder head, cylinder and the crank case were assembled together using four threaded compression rods with nuts and washers not only because the threaded rods were standard parts which only needed to be cut to appropriate length but also accommodate adjustment and ease of disassembling the parts. The 12 volts D.C power source and the portability configuration of the compressor side will make it suitable for use anywhere by putting it in the trunk. 12 volts D.C motor has been chosen because the voltage is readily available on the car battery terminals. It will also be coupled with a pair of crocodile tail clip to ensure firm grip when connected to the battery terminals.



Fig. 1. Type of Tyre Inflation (Mushiri T, et. al.)

**Table 1. List of component parts**

S/N	Component parts	Quantity
15	Electric motor	1
14	Outlet	1
13	Cylinder Head	1
12	Nut	4
11	Stud	4
10	Piston	1
9	Cylinder	1
8	Spur gear	2
7	Connecting Rod	1
6	Small Bolt	4
5	Crank-case cover	1
4	Bearing	2
3	Crankshaft	1
2	Coupling cover	1
1	Crank case	1



**Fig. 2. The assembly view of the 5-min DC inflator with the cylinder head**

## 2.2 Design Considerations

The following factors were considered during the design of the machine:

- a) Simplicity in operation and easy to maintain

- b) Portability and compactness of the machine
- c) Ergonomics
- d) Cost of Fabrication
- e) Material
- f) Safety
- g) Assembly
- h) Reliability

## 2.3 Material Selection Criteria

Reliability of a design is a function of the material used for the design. Whether the design will fail or not during service depends strongly on the material selection. The material has to be properly selected in order to meet the intended aim of the design. The following factors are the key factors considered in selecting the best material for the design:

- a) Mechanical stresses,
- b) Weight,
- c) Cost,
- d) Toughness,
- e) Wear resistance,
- f) Availability of raw material and
- g) The ease of fabrication.

Appropriate engineering materials were chosen to cope with the various load, stress, strain and torque to be experienced by various parts of the machine during operation.

## 2.4 Operating Principle of the Machine

The machine working principle is similar to that of an ordinary reciprocating machine except that, it is powered through 12 V DC motor. Once the machine terminal wires are connected to 12 V battery terminals via crocodile clips. An on/off switch will be depressed on the electric motor connected to the inflator via spur gears. The rotating motion of the crankshaft will be converted to reciprocating motion of the piston via the connecting rod. The shim metal plate used as inlet valve will then experience a negative pressure caused by the vacuum created during the downward movement of the piston. It will deflect a little bit to allow air to rush into the cylinder. Immediately the piston is leaving the bottom dead centre (BDC), the inlet valve will experience an upward force which will close it while the outlet valve will open when the pressure reaches the maximum designated pressure by exerting an upward force which is just sufficient to open the outlet valve. The residual time of the fluid inside the cylinder will strongly be determined by the strength of the outlet valve. The cycle will continue until the pressure gauge senses a certain amount of pressure corresponding with an already set pressure whereby sending a low signal to electric motor controller to turn off.

The summary of results on the design analysis/calculations of various components of the design drawing is presented in Table 2.

## 3. RESULTS AND DISCUSSION

The CAD model of the automobile tyre inflator was subjected to stress analysis to determine the effectiveness of the conceptual design for fabrication. The stress variation, buckling, fatigue and factor of safety analyses on the reciprocating member (piston), and torsional analysis of the crank shaft, which are considered as a critical part, were investigated using Finite Element (FE) modelling tool in Solidworks CAD application software.

### 3.1 Connecting Rod

The choice of material for the component is forged steel. The main objective is to minimize the weight and also to ensure that it will not fail due to Buckling and Fatigue. The Cross sectional area of the I-section connecting rod is considered to be free variable depending on

either mass of the connecting rod due to buckling or fatigue.

In the Finite Element (FE) domain, the solid mesh of the connecting rod was generated by discretizing the connecting rod model into 10125 elements with 16877 nodes and 49770 degrees of freedom as shown in Fig. 3. The load acting on the connecting rod through the piston is estimated to be 155 N. The simulation result indicated that the maximum stress of  $3.7 \times 10^6 \text{ N/m}^2$ , is experienced around the fillet neck of the connecting rod. However, this maximum stress value obtained is lower than the yield strength of the forged steel. The stress distribution on the connecting rod is as shown in Fig. 4.

Furthermore, the resultant displacement of the reciprocating member was assessed under the same load as shown in Fig. 5. A maximum resultant displacement of 0.00092 mm was observed around the small end of the connecting rod. Since the stress value observed around the small end bearing of the connecting rod is below the yield stress as well, the displacement at that area is tolerable within the elastic limit of the selected material which has not been exceeded.

The resistance to buckle of the connecting rod was also assessed by subjecting it to buckling test in order to determine the suitability of the reciprocating member. Fig. 6 shows the resultant displacement of the member after the buckling test has been conducted. The maximum resultant lateral displacement under the axial is 0.02 mm around the big end bearing. From design calculation, the buckling load computed was 755 N, which is the expected load that can cause the connecting rod to buckle. The expected load is far greater than the load that causes 0.02 mm resultant displacement, thus can be considered negligible. Fig. 7 also shows the strain distribution on the connecting rod with a maximum strain of  $1.38 \times 10^{-5}$  which can also be considered negligible based on the same reason given for resultant displacement.

The FE simulation test for Factor of safety (FOS) was conducted in order to determine the integrity of the reciprocating member, the minimum FOS distribution observed was  $1.3 \times 10^2$ . Fig. 8 shows the result obtained for Factor of safety distribution.

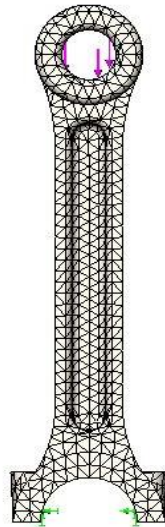


**Fig. 3. Connecting rod solid mesh with normally acting load in the small end bearing**

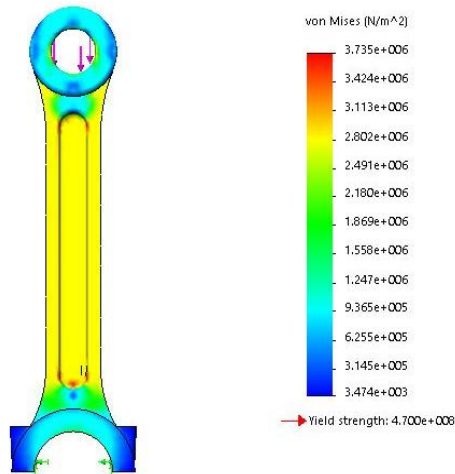


**Fig. 4. Stress distribution on the connecting rod**

In order to validate the effectiveness of the FE simulation runs on the reciprocating member integrity, the factor of safety obtained from design calculation and the maximum stress obtained from the stress distribution was evaluated. With yield strength of  $4.7 \times 10^8 \text{ N.m}^2$  and maximum stress of  $3.7 \times 10^6 \text{ N/m}^2$ , the calculated factor of safety is  $1.3 \times 10^2 \text{ N/m}^2$ , which is the same as the value obtained from the FE simulation run in Fig. 4. Hence, the integrity of the reciprocating member is guaranteed and it is acceptable for fabrication.

### 3.2 Crankshaft

Crankshaft is subjected to both torsional and bending load. With the bore as the DNA, it is easy to design the complex structural geometry of the machine rotating member. Solidworks CAD application is used to modelled the crankshaft based on the parameters obtained during the design analysis.

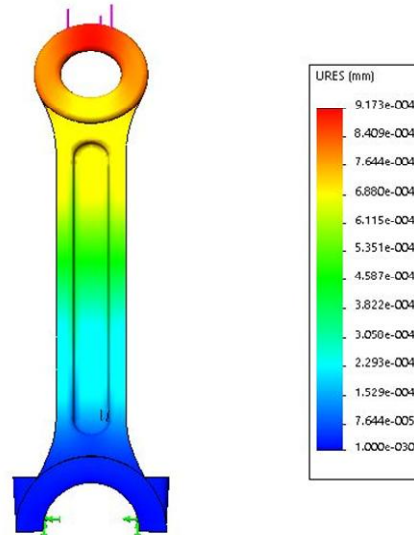


**Fig. 5. Static displacement distribution of the connecting rod**

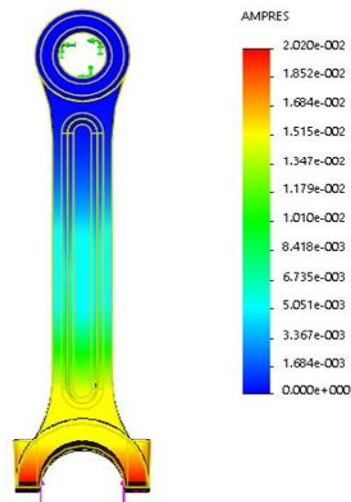


**Fig. 6. Buckling amplitude of the connecting rod**



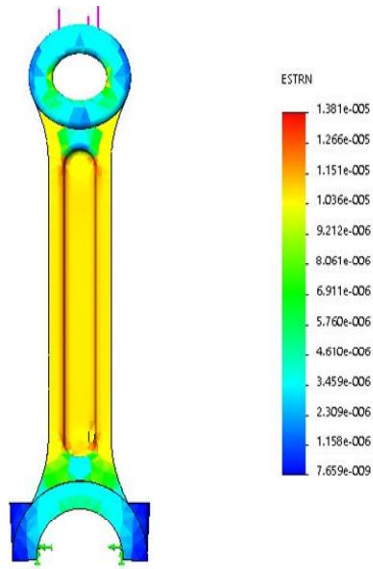


Fig. 7. Strain distribution of the connecting

pin and main journals. However, this maximum stress value obtained is lower than the yield strength of the alloy steel selected as material for the crankshaft.

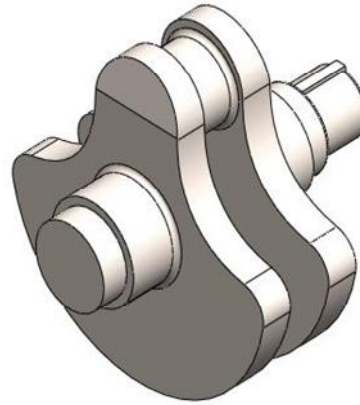


Fig. 9. Crankshaft solid model

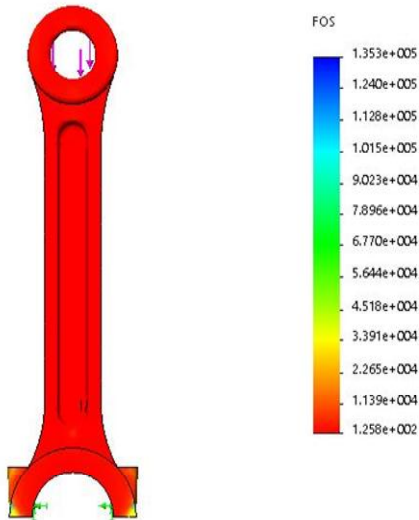


Fig. 8. Factor of safety of the connecting

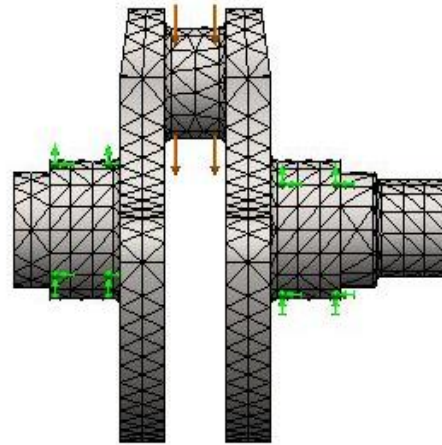


Fig. 10. Crankshaft solid mesh with normally acting force along the crankpin

### 3.3 Bending Analysis

Figs. 9 and 10 show the solid model and the solid mesh of the crank shaft respectively. The solid model was meshed into 15336 nodes with 9362 elements and 44496 degree of freedoms. The simulated FE analysis of the stress distribution in the crankshaft is shown in Fig. 11. The simulation result indicated that the maximum stress of  $2.48 \times 10^6 \text{ N/m}^2$ , is experienced around the fillet neck of the crank-

Furthermore, the resultant displacement of the crankshaft was assessed under the same load as shown in Fig. 12. A maximum resultant displacement of  $9.8 \times 10^{-5} \text{ mm}$  was observed around the crank pin. Since the stress value observed is below the yield stress as well, the displacement at that area is tolerable within the elastic limit of the selected material which has not been exceeded. Fig. 13 also shows the strain distribution on the crankshaft with a maximum strain of  $8.5 \times 10^{-6}$  which can also be

considered negligible based on the same reason given for resultant displacement.

Hence, the integrity of the crankshaft is guaranteed and it is acceptable for fabrication.

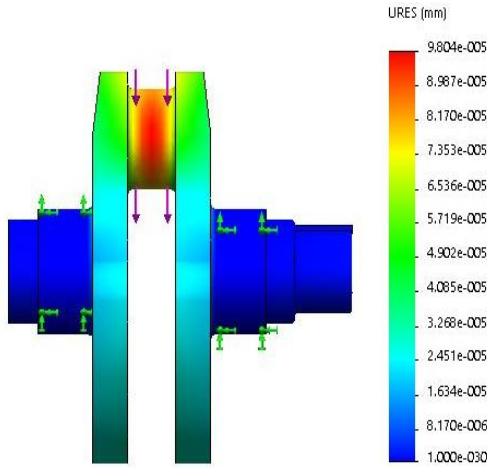


Fig. 11. Stress distribution on the crankshaft

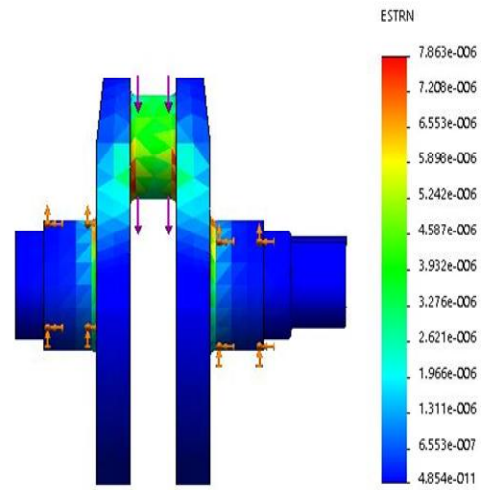


Fig. 13. Strain distribution of the crankshaft

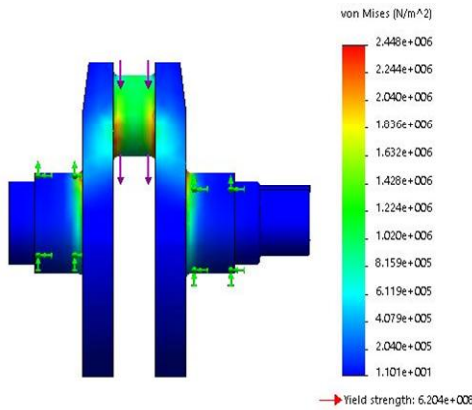


Fig. 12. Static displacement distribution of the crankshaft

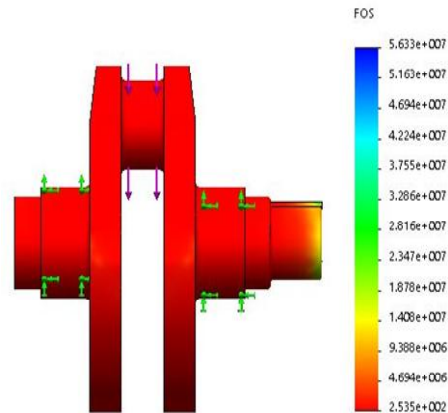


Fig. 14. Factor of safety distribution of the crankshaft

The FE simulation test for Factor of safety was also run in order to determine the integrity of the rotating member, the minimum FOS distribution observed was  $2.5 \times 10^2$ . Fig 14 shows the result obtained for Factor of safety distribution.

The entire finite element simulation results from the stress distribution and resultant displacement variation in the reciprocating members gave an insight to location experiencing maximum stress and maximum displacement. This location of the members is a potential position where failure may likely begin when the machine is fabricated and put to use. However, the maximum stress value was far lower than the yield strength of the corresponding material for the members, which

Validation of the effectiveness of the FE simulation runs was also done for the crankshaft integrity, the factor of safety obtained for the maximum stress obtained from the stress distribution was evaluated. With yield strength of  $6.2 \times 10^8 \text{ N/m}^2$  and maximum stress of  $2.48 \times 10^6 \text{ N/m}^2$ , the calculated factor of safety is  $2.5 \times 10^2$ , which is the same as the value obtained from the FE simulation run in Fig. 4.



**Table 2. Summary of design analysis/ calculations and design values**

S/N	Design factor	Mathematical model	Design values
1	Volume of hollow cylinder of tyre	$V = \pi w(R^2 - r^2)$	.044 $m^3$
2	Density of dry air	$\rho = \frac{P_{max}}{RT}$	2.832 $\frac{kg}{m^3}$
3	The stroke volume	$V_s = \frac{\pi D^2 L}{4}$	17,583 $mm^3$
4	The Clearance volume	$V_c = \frac{\pi D^2 L_c}{4}$	703.325 $mm^2$
5	Minor diameter of stud Of cylinder	$d_c = \sqrt{\frac{D^2 \times P_{max}}{n_s \times \sigma_t}}$	.87 $mm$
6	Piston head thickness	$.433D \sqrt{\frac{P_{max}}{\sigma_{allowable}}}$	1.17 $mm$
7	Thickness of the piston ring	$t_r = D \sqrt{\frac{3P_w}{\sigma_{br}}}$	.804 $mm$
8	Number of the piston rings	$b_r = \frac{D}{10 \times Z}$	$Z = 3.408$
9	Maximum side thrust ( $R_N$ ) of the piston skirt	$R_N = \mu \times \frac{\pi}{4} D^2 P_{max}$	15.49 $N$
10	Length of piston skirt ( $L_{ps}$ )	$R_N = L_{ps} D P_{bc}$	1.436 $mm$
11	Length of piston ( $L_p$ )	$L_p = b_o + Z(b_r) + (Z - 1)b_i + L_{ps}$	6.096 $mm$
12	Maximum gas force ( $f_{gmax}$ ) of piston pin	$F_{gmax} = \frac{\pi}{4} D^2 P_{max}$	155 $N$
13	Length of piston pin in connecting rod bearing ( $L_i$ )	$L_i = .45D$	10.788 $mm$
14	Diameter of piston pin	$d_p = \frac{F_{gmax}}{L_i \times P_b}$	1.44 $mm$
15	Thickness of cylinder head ( $t_n$ )	$t_n = D \sqrt{\frac{c \cdot P_{max}}{\sigma_c}}$	2 $mm$
16	Design of connecting rod (Fatigue consideration)	$M_f = \rho \frac{F}{\sigma_e} L$	.605 $\times 10^{-3} kg$
17	Design of connecting rod (Buckling consideration), $M_b$	$M_b = \left(\frac{12F}{\alpha \pi^2}\right)^{\frac{1}{2}} L^2 \left(\frac{\rho}{E^{\frac{1}{2}}}\right)$	1.59 $\times 10^{-3} kg$
18	Buckling Load, $W_B$	$W_B = \frac{\pi D^2}{4} \times P_{max} \times F_s$	775 $N$
19	Design of Crank shaft (Crank pin diameter), $D_p$	$D_p = (.60 \text{ to } 0.65) \times D$	14.38 $mm$
20	Length of the crank pin, $L_p$	$L_p = (.35 \text{ to } 0.45) \times D$	8.39 $mm$
21	Web thickness, $W_t$	$W_t = .25 \times D$	17.98 $mm$
22	Main journal diameter, $J_d$	$J_d = .75 \times D$	17.98 $mm$

made the minimum factor of safety obtained to be  $1.3 \times 10^2$  for the connecting rod. The buckling Test analysis indicated that the connecting rod will not buckle under the load acting on the piston. This corroborates the slenderness fitness of the machine member, as one of the

objectives of connecting rod design is to reduce the weight of the reciprocating member.

The FE simulation on the crank shaft to investigate bending showed that the alloy steel chosen as the shaft material is adequate, as

obtained maximum stress on the shaft after the simulation did not exceed the material yield strength and a negligible maximum resultant displacement of  $9.8 \times 10^{-5} \text{ mm}$  is experienced by the shaft under the bending load of 155 N. The shaft is expected to be able to withstand a normally acting load that may have resulted from the compresses air pressure. Hence, the crank shaft design is considered appropriate and fit for fabrication.

#### 4. CONCLUSION

In this study, a Five-minute DC powered tyre inflator has been successfully conceptualized and designed. The machine was designed to satisfy a tyre specification of R205/65R15 95H. It has two units, the compressor side and the electric motor side. The compressor side was designed to have piston, crank shaft, cylinder, cylinder head, rings, crank case, valves, pressure gauge and four studs.

The design analysis of the reciprocating parts, connecting rod and crank shaft was done and structural integrity of the members evaluated using FE modelling tool in Solidworks CAD application. Under the action of 155 N load on top of the piston, the simulation result indicates that a maximum stress of  $3.7 \times 10^6 \text{ N/m}^2$  was reached along the fillet neck of the connecting rod, and this value is lower than the yield strength of the material used which is  $4.7 \times 10^8 \text{ N/m}^2$ .

The strength worthiness with respect to slenderness ratio of the connecting rod was confirmed by the buckling analysis with a shape factor of 0.8. Upon the subjection of the crank shaft to a load of 155 N acting normally to the crank pin, the shaft experienced a negligible resultant displacement of  $9.8 \times 10^{-5} \text{ mm}$  and a maximum stress of  $2.48 \times 10^6 \text{ N/m}^2$  with a minimum factor of safety of  $2.5 \times 10^2$  indicating that the crank shaft design is appropriate. The volumetric efficiency is found to be 80% while the working efficiency is 62.5%.

Hence the conceptual design is considered fit for fabrication based on the design analysis and evaluation, it is expected that the machine will fulfil its intended purpose upon fabrication.

#### COMPETING INTERESTS

Authors have declared that no competing interests exist.

#### REFERENCES

1. Bharati VJ, Johny D, Kabiko G, Karthrik K, Mohanraj M. Design and fabrication of automatic tyre inflator and deflation system. *International Journal of Advance Research and Innovation Ideas in Education*. 2016;2(3):302-304.
2. Purwar SK. Automatic tyre inflation system. *International Research Journal of Engineering and Technology*. 2017;4(4): 2384-2387.
3. Hamed M, Tesfa B, Gu F, Ball A. The influence of vehicle tyre pressure on the suspension system response by applying the time-frequency approach. In *Automation and Computing (ICAC)*. 19<sup>th</sup> International Conference on IEEE. 2013;1-6.
4. Vishal PP, Shridhar SJ, Nilesh DD. Performance and analysis of single stage reciprocating air compressor test rig. *International Research Journal of Engineering and Technology*. 2015;2(1): 12-23.
5. Periasamy K, Vijayan S. Design and Development of Air-Less Car Tyre. *International Journal of Advances in Engineering and Technology*. 2014;7(4): 1312-1317.
6. Hemant S, Pratik G. Design of automatic tyre inflation system. *Industrial Science*. 2014;1(4):1-7.
7. Indrajeet B, Suyash K. A survey on automatic air inflating system for automobile. *International Journal of Innovative Research in Science, Engineering and Technology*. 2016;5(10): 18517-18523.
8. Kayisoglu B, Engin Y, Dalmisl S. Developing an automatic tire pressure control system to improve the tractive efficiency of tractors. *Journal of Agricultural Machinery Science*. 2014; 10(3):253-259.
9. Latha OH, Irfan SS, Raheem JA. Solar based air compressor for inflating tyres. *Journal of Mechanical and Civil Engineering*. 2014;11(5):29-33.
10. Mushiri T, Muzhanje AT, Mbohwa C. Design of an automatic tyre pressure inflation system for small vehicles. *Proceedings of the 2016 International Conference on Industrial Engineering and Operations Management Detroit, Michigan, USA*; 1325-1335.

11. Rathi K, Shitole A, Kalhapure S, Pujari BR. Automatic central air inflation system. *Journal of Mechanical and Civil Engineering*. 2017;1-3. production of thin filament coil. *Nigerian Journal of Technology*. 2017;36(2):411-420.
12. Farayibi PK. Finite element analysis of plastic recycling machine designed for the

---

© 2018 Farayibi et al.; This is an Open Access article distributed under the terms of the Creative Commons Attribution License (<http://creativecommons.org/licenses/by/4.0>), which permits unrestricted use, distribution, and reproduction in any medium, provided the original work is properly cited.

*Peer-review history:*  
*The peer review history for this paper can be accessed here:*  
<http://www.sdiarticle3.com/review-history/46575>